Direct electrophysiological measurement of human default network areas

Kai J. Miller[a,b], Kurt E. Weaver[c], and Jeffrey G. Ojemann[d,1]

Departments of [a]Neurobiology and Behavior, [b]Physics, [c]Radiology, and [d]Neurological Surgery, University of Washington School of Medicine, Seattle, WA 98195

Edited by Marcus E. Raichle, Washington University School of Medicine, St. Louis, MO, and approved June 2, 2009 (received for review February 24, 2009)

Neuroimaging-based investigations in humans have established the existence of brain regions that are selectively metabolically active while resting. We report a population-scale neurophysiological measurement of activity in regions of this ''default network,'' by recording high-frequency power (76–200 Hz) electrical potentials directly from these regions in three human subjects. A selective increase observed during only resting, when compared with activity, firmly establishes a neuronal origin for default network phenomena.

cognition | electrocorticography | medial frontal cortex | gamma activity | precuneus

Blood-flow-based imaging technologies, such as positron emission tomography and fMRI, have revealed that a constellation of human brain regions, including the medial prefrontal cortex (MdPFC) and the precuneus, have a distinct rise in activity specifically as individuals disengage from mentally demanding tasks (1). That is, the blood-oxygen-level-dependent (BOLD) signal within a set of regions collectively called the ''default network'' (DN) is specifically elevated in the absence of demanding external interaction (e.g., during task-initiated control periods or scanning in the absence of a specific task, i.e., the ''resting state'') and is suppressed during the execution of cognitive, sensory, or motor processes (2).

This BOLD signal increase during resting has been the primary identifying feature of the DN, and it has been interpreted with the hypothesis that there are robust ongoing neuronal processes in the cortex that are interrupted during engagement in attention-demanding tasks (2, 3). However, resting-state fMRI investigations are intrinsically susceptible to interference from cardiac and respiratory cycles, and because of this, some evidence has questioned the neuronal origins of resting-state default activity (4). Others have proposed that the BOLD signal is physiologically driven, at least in part, by the metabolic demand of a locally coherent ensemble of rapidly oscillating cell assemblies at high frequencies (5). To fully ascertain the contributions of the DN to cognitive and behavioral neuroscience and to the pathophysiology of mental illness (6), a complete characterization of the neurophysiological phenomena that drive DN function is required.

To date, the electrophysiological origins of DN activities have been limited to scalp-based EEG (7). The EEG signal at a given electrode is an average across a large area of cortical tissue (8–11) and particularly limited for buried cortex, such as the MdPFC. A few studies have combined concurrent measurements of EEG and BOLD-fMRI (7, 12–14) with mixed results.

Here, we used electrocorticography (ECoG) measurement in humans undergoing long-term recording from the cortical surface for localization of seizure foci. In some individuals, electrodes had been placed over deep medial cortex, including the MdPFC and the precuneus or posterior cingulate regions. Recordings were obtained during various functional engagement tasks and control periods of rest. In contrast to EEG, ECoG reports a direct measure of local cortical activity (e.g., refs. 15–19). In particular, high-frequency changes (76–200 Hz) in the brain surface electrical potential power spectrum have consistently been demonstrated to reflect activated or engaged cortex (16, 17, 19–22). Accordingly, we anticipated that neuronal population activity, approximated by these electrical changes, might increase within DN regions during control periods of resting fixation and be suppressed during the execution of cognitive or motor computations.

Results

We determined the power in brain surface electric potentials, between 76 and 200 Hz, using ECoG recordings (Fig. 1). Three patients, with intractable seizures, were studied after they had undergone placement of subdural ECoG electrode arrays (including coverage over the MdPFC and precuneus regions) for clinical monitoring. Each individual passively fixated on a distant wall (resting) and then engaged in one or more of three different active behavioral tasks: verb generation, visual target detection, or finger movement. Distributions of power in the 76–200 Hz range during resting and task engagement were compared with identified brain regions with a statistically significant change.

Electrode pairs in the supplemental motor area (Figs. 1 and 2) and primary visual cortex (Fig. 2) illustrate a significant increase in activity associated with finger movement, vision, or speech compared with passive fixation. In each case, an MdPFC electrode pair, however, shows the exact opposite: Neural activity is diminished from resting-state levels while the subject is engaged in a task (Table 1). A precuneus electrode pair showed the same effect in subject 2 (Fig. 2). When the same analysis was applied to other frequency ranges (4–8, 8–12, 15–25, and 28–40 Hz), the only consistent trend was an increase in power between 4 and 8 Hz in the MdPFC with activity (statistically significant only in subject 3).

Discussion

Other studies measuring BOLD-fMRI changes (23, 24) and correlation in electroencephalographic scalp rhythms (7, 25) have demonstrated that these default regions intrinsically fluctuate in concert, giving rise to a cross-regional ''resting-state network.'' Correlated fluctuations also were seen with ECoG comparing distant sensory regions (26).

The results presented here illustrate the direct cortical measurement of changes in the amplitude of population-scale neurophysiology associated with human DN regions and reveal that high levels of electrical brain activity persist specifically in the absence of outside stimulation. This conjugate on/off pattern of ECoG activation, which was consistent across three different active tasks, parallels a vast literature of fMRI inquiry linking DN activity to cognition and behavior (2, 3, 5, 27, 28). These results reveal a neural signature of stimulus-independent activity, refuting alternative hypotheses that attribute resting-state

Author contributions: J.G.O. designed research; K.J.M. and J.G.O. performed research; K.J.M., K.E.W., and J.G.O. analyzed data; and K.J.M., K.E.W., and J.G.O. wrote the paper.

The authors declare no conflict of interest.

This article is a PNAS Direct Submission.

[1]To whom correspondence should be addressed. E-mail: jojemann@u.washington.edu.

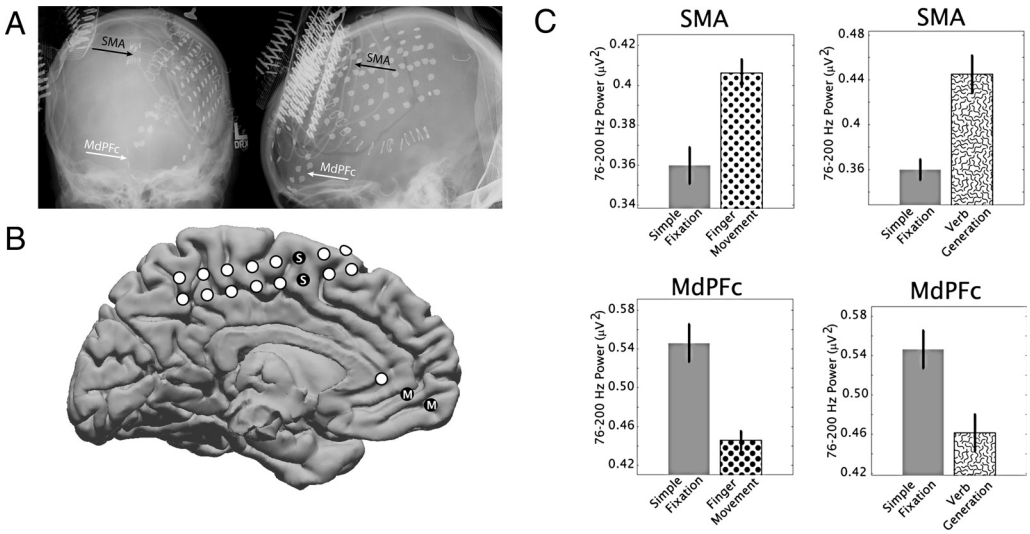

Fig. 1. Subject 1, areas of high-frequency power increases and decreases. (*A*) Electrodes covered the medial frontal (interhemispheric) cortex, and the power level between 76 and 200 Hz in the electrocorticography potential was measured from differential electrode pairs. (*B*) Corresponding locations of electrode pairs in the brain of subject 1 (white and black dots) are shown on a template brain, with coverage of medial prefrontal cortex (MdPFC, ''M'') [electrode pair Talairach (35) locations are shown in Table 1] and supplemental motor area (SMA, ''S'' in black dots). (*C*) The power at 76–200 Hz is shown for resting fixation (solid gray bars), finger movement (dots), and verb generation (squiggles). Power was higher in the SMA with finger movement but lower in the MdPFC during cued finger movement. Error bars indicate the standard error; all differences were significant ($P < 0.01$).

BOLD changes in default regions to nonneuronal artifacts (29, 30). The conclusion of many functional imaging studies that neural activity in MdPFC and the precuneus is specifically increased during rest is concretely validated by these measurements.

Materials and Methods

Subjects and Clinical Procedures. Subdural electrode arrays (Fig. 3) were placed on the cortical surface for extended clinical monitoring and localization of seizure foci in three patients. Patients 1, 2, and 3 were right-handed, 18-, 21-, and 31-years-old, and female, male, and male, respectively. All had medically intractable seizures and were recommended for invasive electrode monitoring with surgery, and electrode placement was determined through comprehensive evaluation at the Regional Epilepsy Center, Harborview Medical Center, University of Washington. Each gave informed consent to participate in an internal-review-board-approved experimental protocol. Experiments were performed at the bedside, using Synamps2 amplifiers (Neuroscan). Data were recorded, and stimuli were presented with a monitor (≈1 m away) using BCI2000 (31). Subdural platinum electrode arrays and strips (2.3-mm diameter exposed, 1-cm interelectrode distance; Ad-Tech) were implanted, and electrode cortical surface positions were localized from X-rays and plotted with the Location on Cortex package (32). The potentials were sampled at 1000 Hz, with respect to a scalp reference and ground (software-imposed filter from 0.15 to 200 Hz).

Tasks. All three patients performed a 3-min fixation task (''resting'' condition), where they stared at a 10-cm static ''×'' on the wall, 3 m away. Default network activity has been demonstrated to be independent of whether an

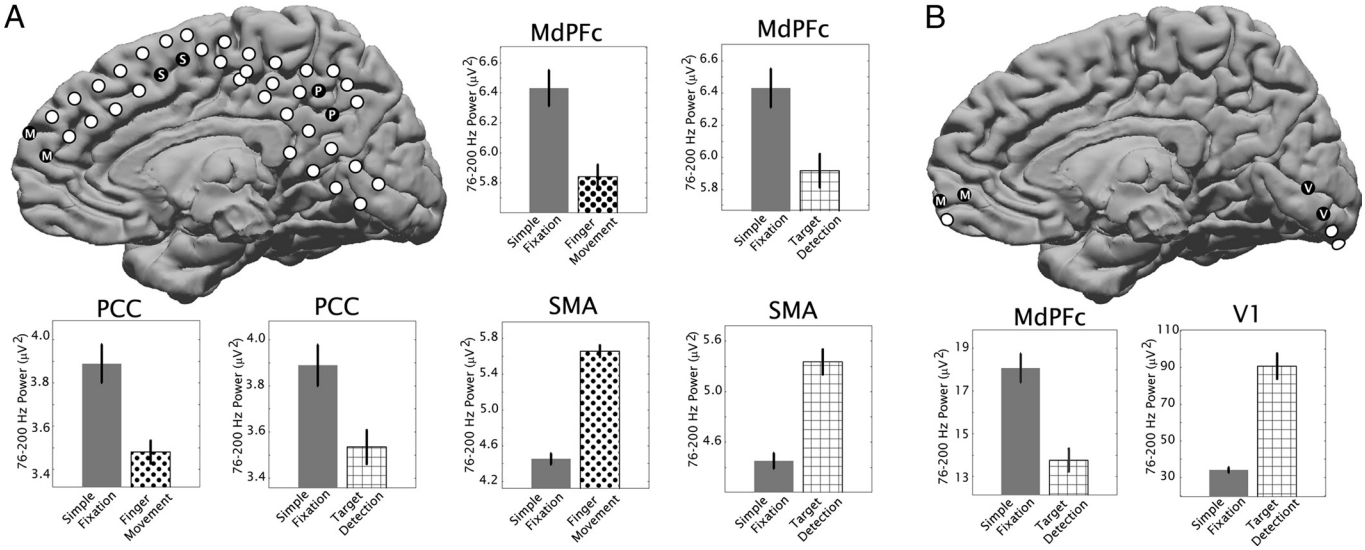

Fig. 2. Power levels between 76 and 200 Hz in the potential measured from differential electrocorticography electrode pairs in subject 2 (*A*) and subject 3 (*B*) are shown for resting fixation (solid gray bars), finger movement (dots), and visual target detection (cross-hatched). Corresponding locations of electrode pairs are shown in schematics, with coverage of MdPFC (''M'') (Talairach locations in Table 1), SMA (''S'' in black dots), posterior cingulate/precuneus cortex (PCC, ''P''), and primary visual cortex (V1, ''V''). Error bars indicate the standard error; all differences were significant ($P < 0.01$).

Table 1. Coordinates for each electrode pair displayed in the figures along with the location and Brodmann area

	Talairach coordinate						
Pair	*x*	*y*	*z*	Lobe	Common name	BA	Change
Sub1–MdPFC	0	44	1	Limbic	Anterior cingulate	ND	Decrease
Sub1–MdPFC	1	54	−3	Frontal	Medial frontal gyrus	10	Decrease
Sub1–SMA	0	−2	60	Frontal	Medial frontal gyrus	6	Increase
Sub1–SMA	−1	0	50	Frontal	Medial frontal gyrus	6	Increase
Sub2–MdPFC	5	62	24	Frontal	Superior frontal gyrus	10	Decrease
Sub2–MdPFC	2	55	16	Frontal	Medial frontal gyrus	9	Decrease
Sub2–SMA	2	11	47	Frontal	Superior frontal gyrus	6	Increase
Sub2–SMA	1	2	53	Frontal	Medial frontal gyrus	6	Increase
Sub2–PCC	2	−54	38	Parietal	Precuneus	7	Decrease
Sub2–PCC	0	−43	41	Limbic	Cingulate gyrus	31	Decrease
Sub3–V1	2	−79	4	Occipital	Lingual gyrus	18	Increase
Sub3–V1	4	−85	−7	Occipital	Lingual gyrus	18	Increase
Sub3–MdPFC	3	58	−1	Frontal	Medial frontal gyrus	10	Decrease
Sub3–MdPFC	4	66	1	Frontal	Superior frontal gyrus	10	Decrease

BA, Brodmann area; Change, direction of change with activity; MdPFC, medial prefrontal cortex; PCC, posterior cingulate/precuneus cortex; SMA, supplemental motor area; V1, primary visual cortex; ND, not defined.

individual's eyes are open, closed, or fixating (33, 34). They were instructed to relax but remain still and blink when needed.

Repetitive Finger Movement. Patients 1 and 2 performed repetitive flexion–extension of either the thumb or the forefinger of the right or left hand (contralateral to electrode location in both cases) in response to random interleaved visual cues on a bedside monitor (1 m away), presented every 3 s, alternating with a 3-s interstimulus interval (ISI; during which time they fixated on the screen). Movement onset was determined from a digital dataglove (5DT).

Verb Generation. Patient 1 performed a verb generation task, where a list of concrete nouns was serially presented (2 s word display, then 1–3 s ISI) on a screen 1 m away, during which time an associated verb would be stated.

Visual Target Detection. Patients 2 and 3 performed an engaged target detection task, with pictures of houses (and faces also for patient 3) presented for 400 ms (ISI of 800 ms) with instructions to respond whether or not the target item matched.

Signal Processing. Nearest-neighbor electrode potential pair difference channels were used to isolate the most local cortical activity. A band-pass (Butterworth) filter for 76–200 Hz (*x*-band, ref. 16) was applied (with notch filters at 60-Hz harmonics for ambient line noise). The power was determined in nonoverlapping 400-ms blocks for a given behavioral condition. The distributions for the resting (fixation) and active blocks were compared using an unpaired *t* test, and the resulting *P* value from each electrode pair was Bonferroni corrected for the total number of pairs. Electrodes in regions of interest determined a priori (MdPFC, precuneus, visual cortex, and supplementary cortex) were based on the task and cortical regions covered by the implanted electrodes. All electrodes included in this study were far (>2.5 cm) from any cortical lesion or epileptic focus.

ACKNOWLEDGMENTS. We appreciate the time and dedication of the patients and staff at Harborview Hospital in Seattle, WA. This work was supported by the National Science Foundation (Grants 0622252 and 0130705).

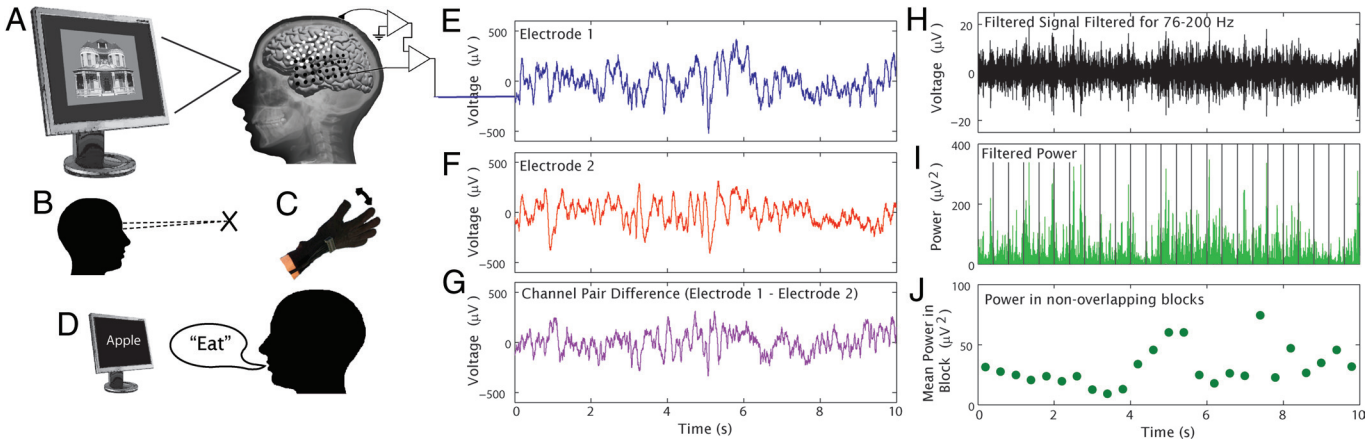

Fig. 3. Summary of methods. (*A*) Subdural electrode arrays were placed on the cortical surface based on clinical considerations. (*B*) A 3-min fixation task served as the resting state. (*C*) Repetitive finger movement. Patients 1 and 2 performed repetitive flexion–extension of either the thumb or the forefinger of the right or left hand in response to random interleaved visual cues. (*D*) Verb generation. Patient 1 performed a verb generation task, where a list of concrete nouns was serially presented on a screen 1 m away, during which time an associated verb would be stated. (*A*) Visual target detection. Patients 2 and 3 performed an engaged target detection task, with pictures of houses (and faces also for patient 3) with vocally reported targets. (*E–J*) Signal processing. Nearest-neighbor electrode potential pair difference channels were used to isolate the most local cortical activity (*A*, *E–G*). A band-pass filter for 76–200 Hz (*x*-band, ref. 16) was applied (*H*) (Butterworth filters, with notch filters at 60 Hz harmonics for ambient line noise). The signal element was squared and summed to obtain the power in nonoverlapping 400-ms blocks (*I* and *J*). The distributions of resting (fixation) and active blocks (mean and standard error shown in Figs. 1 and 2) were compared by using an unpaired *t* test, and the resulting *P* value from each electrode pair was Bonferroni corrected for the total number of medial pairs. Representative pairs are shown, but some others were significant, with increase or decrease clustered by task and region. All electrodes included in this study were far (>2.5 cm) from any cortical lesion or epileptic focus.

1. Raichle ME, et al. (2001) A default mode of brain function. *Proc Natl Acad Sci USA* 98:676–682.
2. Buckner RL, Andrews-Hanna JR, Schacter DL (2008) The brain's default network: Anatomy, function, and relevance to disease. *Ann NY Acad Sci* 1124:1–38.
3. Weissman DH, Roberts KC, Visscher KM, Woldorff MG (2006) The neural bases of momentary lapses in attention. *Nat Neurosci* 9:971–978.
4. Birn RM, Murphy K, Bandettini PA (2008) The effect of respiration variations on independent component analysis results of resting state functional connectivity. *Hum Brain Mapp* 29:740–750.
5. Niessing J, et al. (2005) Hemodynamic signals correlate tightly with synchronized gamma oscillations. *Science* 309:948–951.
6. Broyd SJ, et al. (2009) Default-mode brain dysfunction in mental disorders: A systematic review. *Neurosci Biobehav Rev* 33:279–296.
7. Laufs H (2008) Endogenous brain oscillations and related networks detected by surface EEG-combined fMRI. *Hum Brain Mapp* 29:762–769.
8. Nunez PL (1998) Neocortical dynamics of macroscopic-scale EEG measurements. *IEEE Eng Med Biol Mag* 17:110–117.
9. Nunez PL (2000) Toward a quantitative description of large-scale neocortical dynamic function and EEG. *Behav Brain Sci* 23:371–398.
10. Nunez PL, Silberstein RB (2000) On the relationship of synaptic activity to macroscopic measurements: Does co-registration of EEG with fMRI make sense? *Brain Topogr* 13:79–96.
11. Pfurtscheller G, Neuper C (1992) Simultaneous EEG 10 Hz desynchronization and 40 Hz synchronization during finger movements. *NeuroReport* 3:1057–1060.
12. Laufs H, Daunizeau J, Carmichael DW, Kleinschmidt A (2008) Recent advances in recording electrophysiological data simultaneously with magnetic resonance imaging. *NeuroImage* 40:515–528.
13. Laufs H, et al. (2003) EEG-correlated fMRI of human alpha activity. *NeuroImage* 19:1463–1476.
14. Shmueli K, et al. (2007) Low-frequency fluctuations in the cardiac rate as a source of variance in the resting-state fMRI BOLD signal. *NeuroImage* 38:306–320.
15. Crone NE, Sinai A, Korzeniewska A (2006) High-frequency gamma oscillations and human brain mapping with electrocorticography. *Prog Brain Res* 159:275–295.
16. Miller KJ, et al. (2007) Real-time functional brain mapping using electrocorticography. *NeuroImage* 37:504–507.
17. Miller KJ, et al. (2007) Spectral changes in cortical surface potentials during motor movement. *J Neurosci* 27:2424–2432.
18. Miller KJ, et al. (2008) Beyond the gamma band: The role of high-frequency features in movement classification. *IEEE Trans Biomed Eng* 55:1634–1637.
19. Miller KJ, Zanos S, Fetz EE, den Nijs M, Ojemann JG (2009) Decoupling the cortical power spectrum reveals real-time representation of individual finger movements in humans. *J Neurosci* 29:3132–3137.
20. Ray S, Crone NE, Niebur E, Franaszczuk PJ, Hsiao SS (2008) Neural correlates of high-gamma oscillations (60–200 Hz) in macaque local field potentials and their potential implications in electrocorticography. *J Neurosci* 28:11526–11536.
21. Edwards E, Soltani M, Deouell LY, Berger MS, Knight RT (2005) High gamma activity in response to deviant auditory stimuli recorded directly from human cortex. *J Neurophysiol* 94:4269–4280.
22. Lachaux JP, et al. (2005) The many faces of the gamma band response to complex visual stimuli. *NeuroImage* 25:491–501.
23. Fox MD, Raichle ME (2007) Spontaneous fluctuations in brain activity observed with functional magnetic resonance imaging. *Nat Rev Neurosci* 8:700–711.
24. Raichle ME, Snyder AZ (2007) A default mode of brain function: A brief history of an evolving idea. *NeuroImage* 37:1083–1090.
25. Jann K, et al. (2009) BOLD correlates of EEG alpha phase-locking and the fMRI default mode network. *NeuroImage* 45:903–916.
26. He BJ, Snyder AZ, Zempel JM, Smyth MD, Raichle ME (2008) Electrophysiological correlates of the brain's intrinsic large-scale functional architecture. *Proc Natl Acad Sci USA* 105:16039–16044.
27. Clare Kelly AM, Uddin LQ, Biswal BB, Castellanos FX, Milham MP (2008) Competition between functional brain networks mediates behavioral variability. *NeuroImage* 39:527–537.
28. Luhmann CC, Chun MM, Yi DJ, Lee D, Wang XJ (2008) Neural dissociation of delay and uncertainty in intertemporal choice. *J Neurosci* 28:14459–14466.
29. Kannurpatti SS, Biswal BB (2004) Negative functional response to sensory stimulation and its origins. *J Cereb Blood Flow Metab* 24:703–712.
30. Wise RG, Ide K, Poulin MJ, Tracey I (2004) Resting fluctuations in arterial carbon dioxide induce significant low frequency variations in BOLD signal. *NeuroImage* 21:1652–1664.
31. Schalk G, McFarland DJ, Hinterberger T, Birbaumer N, Wolpaw JR (2004) BCI2000: A general-purpose brain-computer interface (BCI) system. *IEEE Trans Biomed Eng* 51:1034–1043.
32. Miller KJ, et al. (2007) Cortical electrode localization from X-rays and simple mapping for electrocorticographic research: The ''Location on Cortex'' (LOC) package for MATLAB. *J Neurosci Methods* 162:303–308.
33. Fox MD, et al. (2005) The human brain is intrinsically organized into dynamic, anticorrelated functional networks. *Proc Natl Acad Sci USA* 102:9673–9678.
34. Greicius MD, Krasnow B, Reiss AL, Menon V (2003) Functional connectivity in the resting brain: A network analysis of the default mode hypothesis. *Proc Natl Acad Sci USA* 100:253–258.
35. Talairach J, Tournoux P (1988) *Co-planar Stereotaxic Atlas of the Human Brain* (Thieme, New York).